

# Energies, Structures, and Electronic Properties of Molecules in Solution with the C-PCM Solvation Model

MAURIZIO COSSI, NADIA REGA, GIOVANNI SCALMANI, VINCENZO BARONE  
*Dipartimento di Chimica, Università Federico II, Complesso Monte S. Angelo, via Cintia,  
I-80126 Napoli, Italy*

*Received 3 June 2002; Accepted 22 July 2002*

**Abstract:** The conductor-like solvation model, as developed in the framework of the polarizable continuum model (PCM), has been reformulated and newly implemented in order to compute energies, geometric structures, harmonic frequencies, and electronic properties in solution for any chemical system that can be studied *in vacuo*. Particular attention is devoted to large systems requiring suitable iterative algorithms to compute the solvation charges: the fast multipole method (FMM) has been extensively used to ensure a linear scaling of the computational times with the size of the solute. A number of test applications are presented to evaluate the performances of the method.

© 2003 Wiley Periodicals, Inc. J Comput Chem 24: 669–681, 2003

**Key words:** solvation; conductor-like model; C-PCM

## Introduction

Solute-solvent interactions can have dramatic effects on molecular energies, structures, and properties,<sup>1–4</sup> and in many cases such effects can be computed very effectively in the framework of continuum solvation models.<sup>5–7</sup> In these models the bulk of the solvent is represented as a structureless polarizable medium characterized mainly by its dielectric constant  $\epsilon$ . Even when specific interactions require the introduction of some explicit solvent molecules, strongly bound to the solute, the continuum picture is still very useful (and often necessary) to account for long range interactions.

Well-established continuum solvation models exist and are used in many different fields. They are usually based on polarizable dielectrics,<sup>5,6,8</sup> which are perturbed by the solute and generate a suitable reaction field. In addition to such procedures, a conductor-like picture [called conductor-like screening model (COSMO)] was presented some years ago that was developed by several researchers.<sup>9–13</sup> The conductor-like and the dielectric pictures coincide when  $\epsilon \rightarrow +\infty$ , that is, for very polar environments, while the former becomes less accurate for low values of the solvent dielectric constant. On the other hand, in the conductor-like approach the electrostatic problem related to solute-solvent interactions can be solved with a much simpler formalism, which can be useful when very complex systems are studied. In particular, as shown below, first and second derivatives of the molecular free energy with respect to nuclear motions, needed for geometry optimizations and frequency calculations, can be computed with accurate and very efficient algorithms, thanks to the peculiar form

assumed by the electrostatic problem in the conductor-like approach. A different interpretation for the COSMO picture of solvation has also been proposed,<sup>12</sup> which could be generalized to dielectric models too: the computational and algorithmic aspects, however, are quite independent of this debate.

In this article we report on the most recent implementation of this model in the framework of the polarizable continuum model (PCM) formalism, called C-PCM (conductor-like PCM). The PCM is one of the most used and reliable continuum solvation procedures.<sup>8,14</sup> Since its proposal in 1981, it has been continuously updated and extended, and presently it can be used to compute molecular free energies, structures, and properties in any solvent, at the same levels of theory as the corresponding calculations *in vacuo*. State-of-the-art PCM algorithms and implementation are described in detail elsewhere.<sup>15</sup> Here we show to what extent C-PCM can be considered an approximation of the dielectric treatment, comparing the performances of both the approaches.

Moreover, we address the long debated question of the so-called “outlying charge,”<sup>5,8a,9b,13,16</sup> that is, the fraction of solute electronic cloud lying outside the cavity where the solute is placed. This electronic charge actually penetrates the conductor (or the dielectric) medium, and its effects should be accounted for when the reaction field is computed. In previous versions of the conductor-like model, these effects were approximated by resorting to Gauss’ law, exactly as in many dielectric models. On the other

**Correspondence to:** M. Cossi; e-mail: cossi@chemistry.unina.it

Contract/grant sponsor: CIMCF (Centro Interdipartimentale di Metodologie Chimico-Fisiche, University of Naples)

hand, the most recent PCM version takes into account outlying charge effects implicitly, and it does not need any further correction. It has been demonstrated that the conductor-like model can be obtained as the limit for  $\epsilon \rightarrow +\infty$  of this PCM version with implicit inclusion of outlying charge effects.<sup>15,17</sup> This implies that C-PCM results should not be corrected according to Gauss' law, because a better approximation of outlying charge effects is already included in the model as it is.

With modern computational techniques, chemical systems of a few hundreds of atoms are accessible to *ab initio* investigations, and systems of thousands of atoms can be studied with mixed *ab initio*/classical methods. Many calculations on such large molecules exploit procedures based on the fast multipole method (FMM),<sup>18</sup> which allows for the calculation of electrostatic quantities (potentials, fields, etc.) generated by very large charge distributions, with computational times growing linearly with the size of the system. When such molecules are studied in the presence of the solvent, it is important that the performances of the solvation model have the same quality as the corresponding calculations *in vacuo*. We shall see that C-PCM expressions for energies and energy gradients can be easily rearranged in order to use the FMM approach, ensuring a linear growth of the CPU time with the size of the solute. This can be very useful to extend high level calculations of solvent effects also to biochemical and polymeric systems. Moreover, also the preliminary steps of the calculation (namely the formation of the cavity where the solute is accommodated) have been redefined, in order to reduce CPU times and to make this operation linear scaling; another important feature of the new formulation is that the cavity and the pattern of representative points on its surface (see below) have the same symmetry properties as the solute. Such improvements have already been described in an article devoted to the dielectric model (PCM).<sup>15</sup> Here we give only some insights into the improvement of C-PCM performances.

Finally, we remark that PCM and C-PCM equations are designed to describe electrostatic solute-solvent interactions. Other contributions to the molecular free energy in solution can be defined. They are traditionally referred to as cavitation<sup>19</sup> and dispersion-repulsion<sup>20</sup> energies, and they arise respectively from the work needed to form the cavity where the solute is accommodated and from van der Waals interactions with the solvent molecules of the first solvation shells. These contributions are calculated with classical procedures (i.e., they do not enter the molecular Hamiltonian, and affect the solute energy only) described elsewhere.<sup>8d</sup> Such procedures are common to PCM and C-PCM treatments.

The algorithms presented in the following have been implemented in a development version of the GAUSSIAN package,<sup>21</sup> which is expected to be distributed soon to the scientific community.

## Method

As in the other PCM versions, in the C-PCM approach the solute is placed in a cavity formed by the envelope of spheres centered on the atoms or the atomic groups.<sup>22</sup> Inside the cavity the dielectric constant is the same as *in vacuo*, outside it takes the value of the

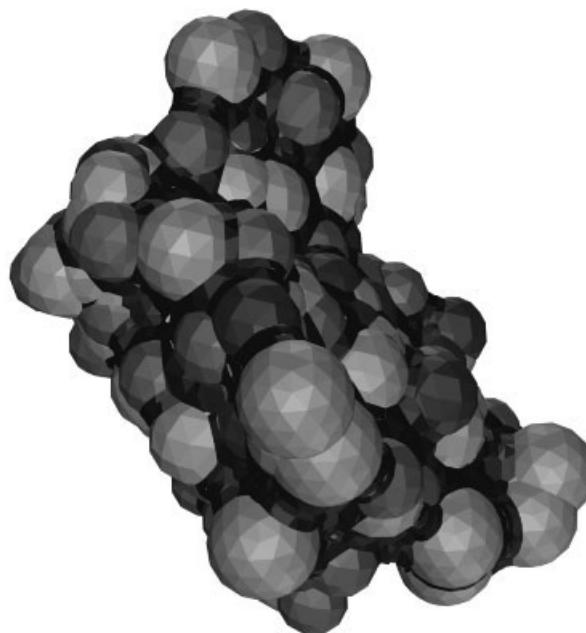


**Figure 1.** Solute cavity for the protein crambin (see Fig. 4), mapped with tesserae of  $0.4 \text{ \AA}^2$  average area.

desired solvent (e.g.,  $\epsilon = 32.6$  for methanol, 78.4 for water, etc.). Once the cavity has been defined, the surface is smoothly mapped by small regions<sup>23</sup> (called tesserae, i.e., small tiles); each tessera is characterized by the position of its center (the “representative point,”  $\mathbf{r}_i$ ), its area ( $a_i$ ), and the vector normal to the surface passing through its center ( $\mathbf{n}_i$ ). These geometric parameters can also be differentiated analytically with respect to nuclear motions.<sup>23</sup> Highly efficient algorithms have been recently developed in order to form such a cavity for very large solutes (several thousands of atoms) with very limited CPU times.<sup>24</sup> An example of cavity, mapped with tesserae of average area of  $0.4 \text{ \AA}^2$  is shown in Figure 1.

The conductor-like reaction field is due to an apparent polarization charge spread on the cavity surface. In practice, the polarization charge is expressed in terms of finite point charges placed in each tessera. For  $\epsilon = +\infty$ , the solvation charges are the solution of the following equation:

$$\mathbf{S}\mathbf{q} = -\mathbf{V} \quad (1)$$

where vectors  $\mathbf{q}$  and  $\mathbf{V}$  collect the solvation charges and the total electrostatic potential generated by solute nuclei and electrons on tesserae, respectively, and matrix  $\mathbf{S}$  elements are<sup>9a,11</sup>

$$\begin{cases} S_{ii} = 1.0694 \sqrt{\frac{4\pi}{a_i}} \\ S_{ij} = \frac{1}{|r_i - r_j|} \end{cases} \quad (2)$$

The quantity  $\mathbf{S}\mathbf{q}$  is the electrostatic potential due to the solvation charges: eq. (1) means that in infinitely polar liquids, the

potential of the solute and that of the charges exactly cancel out on the cavity surface.

In real solvents, with finite dielectric constant, eq. (1) becomes

$$\mathbf{S}\mathbf{q} = -f(\varepsilon)\mathbf{V} \quad (3)$$

The general form for the  $\varepsilon$  dependent factor is  $f(\varepsilon) = \varepsilon - 1/\varepsilon + X$ : in the literature, different values for  $X$  are recommended. In the original COSMO derivation the value  $X = 0.5$  was proposed,<sup>9a</sup> as a compromise between the optimal values for a net charge and a dipole embedded in a spherical cavity. On the other hand, the value  $X = 0$  was preferred in many applications, because it leads to a formal observance of Gauss' law:

$$\sum_i^{\text{tesseræ}} q_i = -\frac{\varepsilon - 1}{\varepsilon} Q_{\text{solute}} \quad (4)$$

where  $Q_{\text{solute}}$  is the solute net charge. As noted above, in the present approach the total charge is no longer required to obey Gauss' law, so that we can choose the  $f(\varepsilon)$  form, which is more convenient computationally.

It is important to note that  $\mathbf{S}$  elements depend on tesseræ parameters in a very simple way, unlike the elements of the corresponding matrices used in PCM.<sup>14g,15</sup> Moreover,  $S_{ij} = S_{ji}$ , and this property is very useful in the following derivations.

The solute-solvent interaction energy is  $E_{\text{int}} = \mathbf{V}^\dagger \mathbf{q} = \sum_i V_i q_i$ , where  $V_i$  is the solute electrostatic potential in tesseræ  $i$ . Because the solvation charges depend on the solute electronic density linearly, it can be shown<sup>8b</sup> that the quantity that is variationally minimized in Hartree-Fock (HF), Kohn-Sham (KS), or multiconfigurational SCF calculations corresponds to a free energy (i.e.,  $E_{\text{int}}$  minus the work spent to create the solvation charges). Then, if  $E^0 = E[\rho^0] + V_{NN}$  is the solute energy *in vacuo*, the free energy in solution is

$$\mathcal{G} = E[\rho] + V_{NN} + \frac{1}{2} \mathbf{V}^\dagger \mathbf{q} = E[\rho] + V_{NN} - \frac{1}{2} f(\varepsilon) \mathbf{V}^\dagger \mathbf{S}^{-1} \mathbf{V} \quad (5)$$

where  $V_{NN}$  is the nuclear repulsion energy,  $\rho^0$  is the electronic density for the molecule *in vacuo*, and  $\rho$  is the density perturbed by the solvent; the last form of eq. (5) is obtained by using eq. (3). These expressions apply to all the variational methods for which an "electronic density" can be defined. Usually  $\rho$  is defined in terms of a density matrix  $\mathbf{P}$  with elements  $P_{\mu\nu}$  based on atomic functions  $\{\chi_\mu\}$ . The Fock matrix (and its KS or MC-SCF generalizations) are corrected by a C-PCM term:

$$\begin{aligned} F_{\mu\nu} &= F_{\mu\nu}^0 + v_{\mu\nu}^{\text{CPCM}} \quad (6) \\ v_{\mu\nu}^{\text{CPCM}} &= -\frac{1}{2} f(\varepsilon) \mathbf{V}_{\mu\nu}^\dagger \mathbf{S}^{-1} \mathbf{V} - \frac{1}{2} f(\varepsilon) \mathbf{V}^\dagger \mathbf{S}^{-1} \mathbf{V}_{\mu\nu} \\ &= -f(\varepsilon) \mathbf{V}^\dagger \mathbf{S}^{-1} \mathbf{V}_{\mu\nu} = \mathbf{q}^\dagger \mathbf{V}_{\mu\nu} \quad (7) \end{aligned}$$

where  $F_{\mu\nu}^0$  is the Fock matrix for the isolated solute, and the uncontracted potential matrix has elements

$$V_{\mu\nu}^i = \int \chi_\mu(\mathbf{r}) \frac{1}{|\mathbf{r} - \mathbf{r}_i|} \chi_\nu(\mathbf{r}) d\mathbf{r} \quad (8)$$

Note that in eq. (7) we used the symmetry of  $\mathbf{S}$  matrix.

Performing geometry optimizations in solution is a very important step in the theoretical study of many chemical systems and processes. To do that efficiently, it is necessary to compute analytically the free energy gradients with respect to nuclear displacements. Differentiating eq. (5) we obtain

$$\frac{\partial \mathcal{G}}{\partial x} = \mathcal{G}^x = E^x[\rho] + V_{NN}^x - \left( \frac{1}{2} f(\varepsilon) \mathbf{V}^\dagger \mathbf{S}^{-1} \mathbf{V} \right)^x \quad (9)$$

where the first two contributions are formally identical to those computed *in vacuo* (but using the electronic density perturbed by the solvent), and all the terms depending on the density derivatives have been avoided, as usual.<sup>25</sup> Because

$$(\mathbf{S}^{-1})^x = -\mathbf{S}^{-1} \mathbf{S}^x \mathbf{S}^{-1} \quad (10)$$

the C-PCM explicit contribution to free energy gradients is

$$\begin{aligned} -\frac{1}{2} f(\varepsilon) (\mathbf{V}^\dagger \mathbf{S}^{-1} \mathbf{V})^x &= -\frac{1}{2} f(\varepsilon) (\mathbf{V}^\dagger)^x \mathbf{S}^{-1} \mathbf{V} - \frac{1}{2} f(\varepsilon) \mathbf{V}^\dagger \mathbf{S}^{-1} \mathbf{V}^x \\ &\quad + \frac{1}{2} f(\varepsilon) \mathbf{V}^\dagger \mathbf{S}^{-1} \mathbf{S}^x \mathbf{S}^{-1} \mathbf{V} \\ &= (\mathbf{V}^\dagger)^x \mathbf{q} + \frac{1}{2f(\varepsilon)} \mathbf{q}^\dagger \mathbf{S}^x \mathbf{q} \quad (11) \end{aligned}$$

where we have repeatedly used eq. (3) and the symmetry of  $\mathbf{S}$  matrix. The C-PCM contribution is then easily computed in terms of solute potential derivatives, solvation charges, and the derivatives of  $\mathbf{S}$ , which are simple functions of tesseræ geometric derivatives:

$$\begin{cases} S_{ii}^x = -\frac{1}{2} S_{ii} \frac{a_i^x}{a_i^2} \\ S_{ij}^x = -\frac{1}{|\mathbf{r}_i - \mathbf{r}_j|^3} [(\mathbf{r}_i - \mathbf{r}_j) \cdot \mathbf{r}_i^x - (\mathbf{r}_i - \mathbf{r}_j) \cdot \mathbf{r}_j^x] \end{cases} \quad (12)$$

Note that any reference to the inverse matrix  $\mathbf{S}^{-1}$  is avoided, so that eq. (11) can be applied also when the solvation charges are found by iterative procedures (see below), that is, for very large solutes.

To compute second derivatives in solution, that is,  $\partial^2 \mathcal{G} / \partial x \partial y \equiv \mathcal{G}^{x,y}$ , different C-PCM contributions have to be accounted for. First, the Fock matrix derivatives must be computed (also in this step, any electronic density derivative is avoided):

$$(F_{\mu\nu})^x = (F_{\mu\nu}^0)^x + (v_{\mu\nu}^{\text{CPCM}})^x \quad (13)$$

The first term on the right hand side of eq. (13) is the same as *in vacuo*, while the C-PCM contribution is

$$\begin{aligned}
(\mathbf{v}_{\mu\nu}^{\text{CPCM}})^x &= -\frac{1}{2}f(\varepsilon)[\mathbf{V}^\dagger\mathbf{S}^{-1}\mathbf{V}_{\mu\nu}]^x = -\frac{1}{2}f(\varepsilon)(\mathbf{V}^\dagger)^x\mathbf{S}^{-1}\mathbf{V}_{\mu\nu} \\
&+ \frac{1}{2}f(\varepsilon)\mathbf{V}^\dagger\mathbf{S}^{-1}\mathbf{S}^x\mathbf{S}^{-1}\mathbf{V}_{\mu\nu} - \frac{1}{2}f(\varepsilon)\mathbf{V}^\dagger\mathbf{S}^{-1}(\mathbf{V}_{\mu\nu})^x \\
&= -\frac{1}{2}[\mathbf{S}^x\mathbf{q} + f(\varepsilon)\mathbf{V}^x]^\dagger\mathbf{S}^{-1}\mathbf{V}_{\mu\nu} + \mathbf{q}^\dagger(\mathbf{V}_{\mu\nu})^x \quad (14)
\end{aligned}$$

which contains known quantities only. Then the electronic density must be differentiated also. This is done in the so-called coupled-perturbed (CP) procedure, the key step of which is the definition of a Fock-like matrix, contracted with the density derivative  $F_{\mu\nu}(\mathbf{P}^x)$ . The same C-PCM operator used to correct the Fock matrix [eq. (7)] is used also in CP procedures, contracted with  $\mathbf{P}^x$ :

$$\mathbf{v}_{\mu\nu}^{\text{CPCM}}(\mathbf{P}^x) = -f(\varepsilon)\mathbf{V}^\dagger(\mathbf{P}^x)\mathbf{S}^{-1}\mathbf{V}_{\mu\nu} = -f(\varepsilon)\sum_{\sigma\tau}P_{\sigma\tau}^x(\mathbf{V}^\dagger_{\sigma\tau}\mathbf{S}^{-1}\mathbf{V}_{\mu\nu}) \quad (15)$$

where  $P_{\sigma\tau}^x$  is an element of the density matrix derivative on the basis of atomic functions.

Finally, one has to account for the explicit C-PCM contribution. Differentiating eq. (11) further

$$\begin{aligned}
-\frac{1}{2}f(\varepsilon)(\mathbf{V}^\dagger\mathbf{S}^{-1}\mathbf{V})^{x,y} &= \left[ (\mathbf{V}^\dagger)^x\mathbf{q} + \frac{1}{2f(\varepsilon)}\mathbf{q}^\dagger\mathbf{S}^x\mathbf{q} \right]^y \\
&= (\mathbf{V}^\dagger)^{x,y}\mathbf{q} + \frac{1}{2f(\varepsilon)}\mathbf{q}^\dagger\mathbf{S}^{x,y}\mathbf{q} + (\mathbf{V}^\dagger)^x\mathbf{q}^y \\
&+ \frac{1}{2f(\varepsilon)}(\mathbf{q}^\dagger)^y\mathbf{S}^x\mathbf{q} + \frac{1}{2f(\varepsilon)}\mathbf{q}^\dagger\mathbf{S}^x\mathbf{q}^y \\
&= (\mathbf{V}^\dagger)^{x,y}\mathbf{q} + \frac{1}{2f(\varepsilon)}\mathbf{q}^\dagger\mathbf{S}^{x,y}\mathbf{q} \\
&+ (\mathbf{V}^\dagger)^x\mathbf{q}^y + \frac{1}{f(\varepsilon)}\mathbf{q}^\dagger\mathbf{S}^x\mathbf{q}^y \\
&= (\mathbf{V}^\dagger)^{x,y}\mathbf{q} + \frac{1}{2f(\varepsilon)}\mathbf{q}^\dagger\mathbf{S}^{x,y}\mathbf{q} \\
&+ \frac{1}{f(\varepsilon)}[\mathbf{S}^x\mathbf{q} + f(\varepsilon)\mathbf{V}^x]\mathbf{q}^y \quad (16)
\end{aligned}$$

Differentiating eq. (3) one obtains  $\mathbf{q}^y = -\mathbf{S}^{-1}[\mathbf{S}^y\mathbf{q} + f(\varepsilon)\mathbf{V}^y]$ , so that

$$\begin{aligned}
-\frac{1}{2}f(\varepsilon)(\mathbf{V}^\dagger\mathbf{S}^{-1}\mathbf{V})^{x,y} &= (\mathbf{V}^\dagger)^{x,y}\mathbf{q} + \frac{1}{2f(\varepsilon)}\mathbf{q}^\dagger\mathbf{S}^{x,y}\mathbf{q} \\
&- \frac{1}{f(\varepsilon)}[\mathbf{S}^x\mathbf{q} + f(\varepsilon)\mathbf{V}^x]^\dagger\mathbf{S}^{-1}[\mathbf{S}^y\mathbf{q} + f(\varepsilon)\mathbf{V}^y] \quad (17)
\end{aligned}$$

All the terms in eq. (17) have already been computed, except  $(\mathbf{V}^\dagger)^{x,y}$ , which is provided by usual *ab initio*, semiempirical, and classical programs, and  $\mathbf{S}^{x,y}$ , the form of which is reported below.

$$S_{ii}^{yy} = \frac{3}{4}\frac{S_{ii}}{a_i^2}a_i^x a_i^y - \frac{1}{2}\frac{S_{ii}}{a_i}a_i^{xy} \quad (18)$$

$$\begin{aligned}
S_{ij}^{yy} &= -\frac{1}{|r_i - r_j|^3}[\mathbf{r}_i^x \cdot \mathbf{r}_i^y - \mathbf{r}_i^x \cdot \mathbf{r}_j^y - \mathbf{r}_j^x \cdot \mathbf{r}_i^y + \mathbf{r}_j^x \cdot \mathbf{r}_j^y] \\
&+ \frac{3}{|r_i - r_j|^5}[(\mathbf{r}_i^x \cdot \mathbf{r}_{ij})(\mathbf{r}_i^y \cdot \mathbf{r}_{ij}) - (\mathbf{r}_i^x \cdot \mathbf{r}_{ij})(\mathbf{r}_j^y \cdot \mathbf{r}_{ij}) \\
&- (\mathbf{r}_j^x \cdot \mathbf{r}_{ij})(\mathbf{r}_i^y \cdot \mathbf{r}_{ij}) + (\mathbf{r}_j^x \cdot \mathbf{r}_{ij})(\mathbf{r}_j^y \cdot \mathbf{r}_{ij})] \\
&- \frac{1}{|r_i - r_j|^3}[\mathbf{r}_i^{xy} \cdot \mathbf{r}_{ij} - \mathbf{r}_j^{xy} \cdot \mathbf{r}_{ij}] \quad (19)
\end{aligned}$$

where we have put for simplicity  $\mathbf{r}_{ij} = (\mathbf{r}_i - \mathbf{r}_j)$ .

Note that  $\mathbf{S}^{x,y}$  involves the second derivatives of tesserae geometric elements: in the present implementation these quantities are computed by numerical differentiation of the corresponding gradients (this is done automatically by the program, which builds different cavities along the nuclear displacements and estimates the second derivatives very efficiently). Work is in progress to develop and code the algorithms for the analytic calculation of the geometric second derivatives. Nonetheless, the present procedure has been tested on a great number of systems and has proved completely stable and reliable even for very large solutes.

In molecular mechanics (MM) calculations, only the explicit C-PCM contribution to second derivatives has to be considered. Because MM is usually employed for very large systems, it is convenient to avoid any reference to the inverse  $\mathbf{S}^{-1}$  matrix in order to use the iterative approach described below. Then, in this case we revert to eq. (16), where the explicit charge derivatives  $\mathbf{q}^y$  can be calculated with the procedure presented in the Iterative Solution section.

## Electronic Properties

As said above, the presence of the C-PCM operator in the Fock matrix [eq. (7)] results in a polarization of the solute electronic density. This has a direct effect on all the electronic properties, like the charge distribution, the molecular dipole moment, the spin population, and so on.

However, other solvent contributions must be included in order to calculate those properties that depend not only on the density, but also on the density *derivatives* with respect to some parameters. For example, excitation energies can be computed by time-dependent approaches [usually called random phase approximation (RPA) in Hartree-Fock, and TD-DFT in density functional theory].<sup>26–28</sup> Such procedures are based on the computation of electronic density derivatives with respect to an external electric field. In this case, the C-PCM contribution has the same form of that used for  $\mathcal{G}^{x,y}$  [eq. (15)], where the density is differentiated with respect to nuclear positions to evaluate harmonic force constants.

However, when vertical transitions are considered (i.e., fast electronic transitions, occurring without any change in the nuclear positions), one has to account also for the finite relaxation times of the solvent reaction field, introducing the so-called nonequilibrium

solvation.<sup>29–31</sup> As explained for example in ref. 31, the solvation phenomena arise from different sources. A part of the reaction field is due to the polarization of solvent electron clouds, while the rest is due to the orientation of solvent molecules. The former contribution can rearrange quickly enough to stay in equilibrium with the solute even during vertical transitions; the latter contribution, on the contrary, remains “frozen” during such transitions. In PCM framework the nonequilibrium effects are accounted for by using a different dielectric constant. The preferred choice is the so-called optical constant,  $\epsilon_{\text{opt}} = n^2$ , where  $n$  is the solvent refractive index. Then, the C-PCM effect on vertical transitions can be computed by substituting  $\epsilon$  with  $\epsilon_{\text{opt}}$  in the factor  $f(\epsilon)$  in eq. (15), as detailed in ref. 31.

Also, the calculation of NMR parameters, for example, the nuclear magnetic shieldings, with the GIAO approach<sup>32</sup> depends both on the solute density polarization, and on a C-PCM term to be included in the routines where the magnetic field perturbation is computed. Essentially, the solvation charges behave like “external” charges fixed on the cavity surface. In this case, equilibrium solvation (i.e., the usual dielectric constant  $\epsilon$ ) is required.

Notice that in some implementations of the conductor-like model, the solvent effect on electronic excitations is computed considering only the solute density polarization and ignoring the solvent contribution to the magnetic perturbation, mentioned in the previous paragraph. This is not correct from the theoretical point of view, and it can result in severe numerical errors, as shown below in the section Test Applications.

## Iterative Solution

The inversion procedure needed to obtain the  $\mathbf{S}^{-1}$  matrix becomes too expensive when the number of tesserae increases over a few thousands. In this case it is convenient to switch to an iterative solution of the system:

$$\mathbf{S}\mathbf{q} = -f(\epsilon)\mathbf{V} \quad (20)$$

The straightforward solution of system 20 is, at iteration  $n$

$$q_i^{(n)} = -\frac{1}{S_{ii}} \left[ f(\epsilon)V_i + \sum_{j \neq i} \frac{q_j^{(n-1)}}{|r_i - r_j|} \right] \quad (21)$$

where the  $i$ th charge depends on the solute potential and on the potential generated by all the other charges at iteration  $(n - 1)$ : the initial guess can be chosen, for example, as the diagonal solution

$$q_i^{(0)} = -\frac{f(\epsilon)}{S_{ii}} V_i \quad (22)$$

Unfortunately, this simple approach leads to serious convergence problems for many solutes. From this point of view, C-PCM performs worse than PCM, which has an iterative version that usually converges much faster. The reason is clearly related to the different scaling of long-range interactions between the solvation

charges (roughly proportional to  $|r_i - r_j|^{-3}$  for PCM and to  $|r_i - r_j|^{-1}$  for C-PCM).

Then we have coded different improved convergence schemes for C-PCM, based on DIIS (direct inversion of the iterative subspace) and on conjugate gradients (CG) procedures. In the former approach, described for general PCM equations for example, in ref. 33, the  $i$ th charge at iteration  $n$  no longer depends on the  $q_j^{(n-1)}$ 's, but rather on linear combinations of the  $q_j$ 's coming from several previous iterations, with weights obtained by a least-squares procedure.<sup>33</sup>

The CG scheme, on the other hand, has been implemented following the procedure illustrated in ref. 34 for a general case. In this approach, the charges are updated at each iteration along some “search directions”:

$$\mathbf{q}^{(n)} = \mathbf{q}^{(n-1)} + \alpha_n \mathbf{p}^{(n)} \quad (23)$$

The directions  $\mathbf{p}^{(n)}$  and the coefficient  $\alpha_n$  are optimized by a standard procedure,<sup>34</sup> where the key step is the evaluation of  $\mathbf{S}\mathbf{p}^{(n)}$ , corresponding to the electrostatic potential generated by the pseudo-charges  $\mathbf{p}^{(n)}$ . This quantity can be computed with the FMM procedure<sup>18</sup> (see below).

It is well known that CG performances can be greatly enhanced by preconditioning the system, especially when a large number of coupled linear equations are involved.<sup>34</sup> This means that, instead of system 20, we solve (iteratively) the system

$$\mathbf{M}^{-1}\mathbf{S}\mathbf{q} = -f(\epsilon)\mathbf{M}^{-1}\mathbf{V} \quad (24)$$

where  $\mathbf{M}$  is a proper “approximation” to the  $\mathbf{S}$  matrix, easy to invert. Choosing the suitable preconditioning is a rather technical issue. We defer to a forthcoming article the complete analysis of the different cases that can occur; some examples are cited below, comparing the performances of DIIS and some preconditioned CG approaches.

The same approach can be used to obtain the charge derivatives needed in MM second derivatives [eq. (16)]: differentiating eq. (20) we get the following system

$$\mathbf{S}\mathbf{q}^x = -f(\epsilon)\mathbf{V}^x - \mathbf{S}^x\mathbf{q} \quad (25)$$

so that the  $i$ th charge derivative at iteration  $n$  is

$$q_i^{x,(n)} = -\frac{1}{S_{ii}} \left[ f(\epsilon)V_i^x + S_{ii}^x q_i + \sum_{j \neq i} S_{ij}^x q_j + \sum_{j \neq i} S_{ij} q_j^{x,(n-1)} \right] \quad (26)$$

This system can be solved iteratively with the same techniques as above: as a general rule, many elements of  $\mathbf{q}^x$  are small, and the convergence of system 26 is usually easier than that of 21. A different linear scaling iterative scheme, based on CG approach and supported by a previous version of the FMM (vide infra), was developed by York et al.<sup>35</sup> and implemented in MOPAC for COSMO solvation model. The performances of such an approach are satisfactory with respect to the matrix inversion procedure, though it is limited to the calculation of energies. On the other hand, the procedure illustrated in the present work ensures a linear

scaling procedure for both energies and gradients, which is highly desirable to perform reliable calculations on large molecular systems.

### Linear Scaling

When the iterative scheme has been set up, in order to obtain a procedure whose computational time grows linearly with the solute size, any double loop on the surface tesserae must be avoided. Instead, one can resort to the FMM approach,<sup>18</sup> which can be fruitfully used to compute the electrostatic potential and the electric field generated by the solvation charges whenever they are needed in C-PCM (presently this is limited to energies and gradients). In our implementation we exploited the FMM algorithm recently coded in the development version of Gaussian.

For C-PCM energies, the second term on the right hand side of eq. (21) is the potential generated by all the other charges on tessera  $i$ , and it can be straightforwardly calculated by FMM. The C-PCM contribution to free energy gradients [eq. (11)] contains two terms. The first one,  $(\mathbf{V}^\dagger)^x \mathbf{q}$ , is easily computed in *ab initio* procedures that are able to provide the potential gradients (these procedures usually exploit the FMM approach when the number of atoms is sufficiently high). On the other hand, when force-field based classical methods are used, this term becomes

$$\begin{aligned} (\mathbf{V}^\dagger)^x \mathbf{q} &= \sum_i^{\text{tesserae}} q_i \frac{\partial}{\partial x} \left( \sum_n^{\text{atoms}} \frac{z_n}{|\mathbf{r}_n - \mathbf{r}_i|} \right) \\ &= - \sum_i \sum_n q_i \frac{(\mathbf{r}_n - \mathbf{r}_i) \cdot (\mathbf{r}_n^x - \mathbf{r}_i^x)}{|\mathbf{r}_n - \mathbf{r}_i|^3} z_n \\ &= - \sum_n z_n \left( \sum_i q_i \frac{\mathbf{r}_n - \mathbf{r}_i}{|\mathbf{r}_n - \mathbf{r}_i|^3} \right) \cdot \mathbf{r}_n^x \\ &\quad - \sum_i q_i \left( \sum_n z_n \frac{\mathbf{r}_i - \mathbf{r}_n}{|\mathbf{r}_n - \mathbf{r}_i|^3} \right) \cdot \mathbf{r}_i^x \\ &= - \sum_n z_n \mathbf{E}_n(\mathbf{q}) \cdot \mathbf{r}_n^x - \sum_i q_i \mathbf{E}_i(\mathbf{z}) \cdot \mathbf{r}_i^x \end{aligned} \quad (27)$$

where  $z_n$  is the  $n$ th atomic charge,  $\mathbf{r}_n$  its position, and  $\mathbf{E}(\mathbf{q})$  and  $\mathbf{E}(\mathbf{z})$  are the electric field due to solvation charges in the atomic positions and the electric field due to atomic charges in the tesserae, respectively. These electric fields can be computed by the FMM procedure.

The second C-PCM contribution to gradients is proportional to the quantity

$$\mathbf{q}^\dagger \mathbf{S}^x \mathbf{q} = \sum_{ij} q_i S_{ij}^x q_j = \sum_i q_i S_{ii}^x q_i + \sum_i \sum_{j \neq i} q_i S_{ij}^x q_j \quad (28)$$

The only quadratic loop is contained in the second sum, which can be rearranged by noting that [see eq. (12)]

$$S_{ij}^x = - \frac{(\mathbf{r}_i - \mathbf{r}_j)}{|\mathbf{r}_i - \mathbf{r}_j|^3} \cdot \mathbf{r}_i^x - \frac{(\mathbf{r}_j - \mathbf{r}_i)}{|\mathbf{r}_i - \mathbf{r}_j|^3} \cdot \mathbf{r}_j^x$$

so that

$$\begin{aligned} \sum_i \sum_{j \neq i} q_i S_{ij}^x q_j &= - \sum_i q_i \left( \sum_{j \neq i} q_j \frac{(\mathbf{r}_i - \mathbf{r}_j)}{|\mathbf{r}_i - \mathbf{r}_j|^3} \right) \cdot \mathbf{r}_i^x \\ &\quad - \sum_j q_j \left( \sum_{i \neq j} q_i \frac{(\mathbf{r}_j - \mathbf{r}_i)}{|\mathbf{r}_i - \mathbf{r}_j|^3} \right) \cdot \mathbf{r}_j^x \\ &= -2 \sum_i q_i \left( \sum_{j \neq i} q_j \frac{(\mathbf{r}_i - \mathbf{r}_j)}{|\mathbf{r}_i - \mathbf{r}_j|^3} \right) \cdot \mathbf{r}_i^x \\ &= -2 \sum_i q_i \mathbf{E}_i(\mathbf{q}) \cdot \mathbf{r}_i^x \end{aligned} \quad (29)$$

where  $\mathbf{E}_i(\mathbf{q})$  is the electric field generated in tessera  $i$  by all the other solvation charges. Again, this quantity is easily provided by FMM procedure. In conclusion, all the C-PCM contributions to energies and gradients can be computed with linear scaling procedures, both in quantum mechanical and in classical calculations.

When the charge derivatives  $\mathbf{q}^x$  are calculated with eq. (26), two loops must be processed in order to scale linearly. One of them, namely  $\sum_{j \neq i} S_{ij} q_j^x$ , is simply the potential due to the charge derivatives at the preceding iteration. The second loop is more involved, and it can be rearranged as follows:

$$\begin{aligned} \sum_{j \neq i} S_{ij}^x q_j &= - \sum_{j \neq i} q_j \frac{(\mathbf{r}_i - \mathbf{r}_j)}{|\mathbf{r}_i - \mathbf{r}_j|^3} \cdot \mathbf{r}_i^x + \sum_{j \neq i} \frac{(\mathbf{r}_i - \mathbf{r}_j)}{|\mathbf{r}_i - \mathbf{r}_j|^3} \cdot \mathbf{r}_j^x q_j \\ &= - \mathbf{E}_i(\mathbf{q}) \cdot \mathbf{r}_i^x + \sum_{\lambda=x,y,z} \sum_{j \neq i} \frac{(\mathbf{r}_i - \mathbf{r}_j)_\lambda}{|\mathbf{r}_i - \mathbf{r}_j|^3} (\mathbf{r}_j^x)_\lambda q_j \\ &= - \mathbf{E}_i(\mathbf{q}) \cdot \mathbf{r}_i^x + \sum_{\lambda=x,y,z} E_{i,\lambda}(\mathbf{p}_\lambda) \end{aligned} \quad (30)$$

Here, the first term is simply the electric field due to the charges; for the second term, we have separated the components of the scalar product, obtaining the sum of the  $\lambda$  components of the electric fields generated by the pseudo charges  $p_{\lambda,j} = (\mathbf{r}_j^x)_\lambda q_j$ , for  $\lambda = x, y, z$ . This can be computed by three successive applications of the usual FMM procedure.

### Test Applications

We have said above that the conductor-like approach can be seen as a limit of dielectric solvation models for very polar liquids. In this sense, using eq. (3) for finite values of  $\epsilon$  is an approximation. To estimate how good such an approximation is, and to find the best expression for  $f(\epsilon) = \epsilon - 1/\epsilon + X$ , we have computed the solvation free energy (i.e., the difference between the C-PCM free energy and the energy *in vacuo* at the same level) for a number of small organic molecules (35 neutral and 18 ionic; the set of test

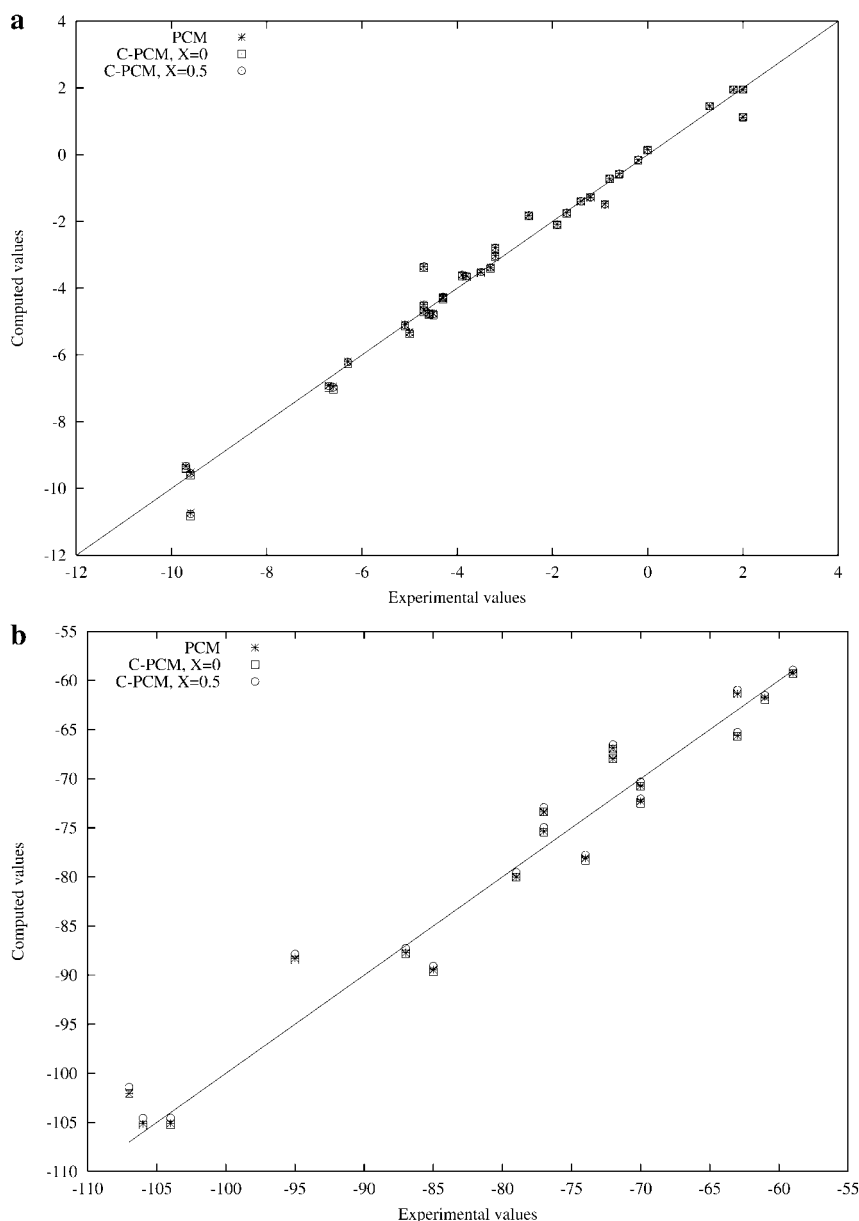


**Figure 2.** Solvation free energy in water for neutral (a) and ionic (b) organic and inorganic solutes, computed at the HF/6-31+G(d) level with PCM and C-PCM procedures and different  $X$  values, compared to experimental results.

solutes is the same as that reported in Tables 3 and 4 of ref. 15), including also nonelectrostatic contributions. The calculations have been performed at the HF level with the 6-31+G(d) basis set,<sup>36</sup> which is known to provide reliable results for this kind of calculation both for neutral and for charged solutes, at the solute geometries optimized *in vacuo*.

In Figure 2 we show the agreement between C-PCM hydration free energies using  $X = 0$  and  $X = 0.5$  with the corresponding PCM values (using the dielectric model described in ref. 15) and with the experimental values for neutral and charged solutes. In Figure 3 the comparison between conductor-like and dielectric

models is repeated in carbon tetrachloride ( $\epsilon = 2.23$ ), with  $X = 0, 0.25, 0.5$ .

We repeated the calculations at the density functional theory (DFT) level using the PBE0 functional<sup>37</sup> with the same basis set. The correlation between PCM and C-PCM calculations is exactly the same as in HF. Note that with both the dielectric and the conductor models the DFT hydration energies are in poor agreement with the experiment, because the size of the solute cavities has been optimized for HF calculations.<sup>38</sup> Anyway, the PCM/experimental discrepancy is quite small (on average 0.47 kcal/mol for neutral, and 1.67 kcal/mol for charged solutes), and it does not

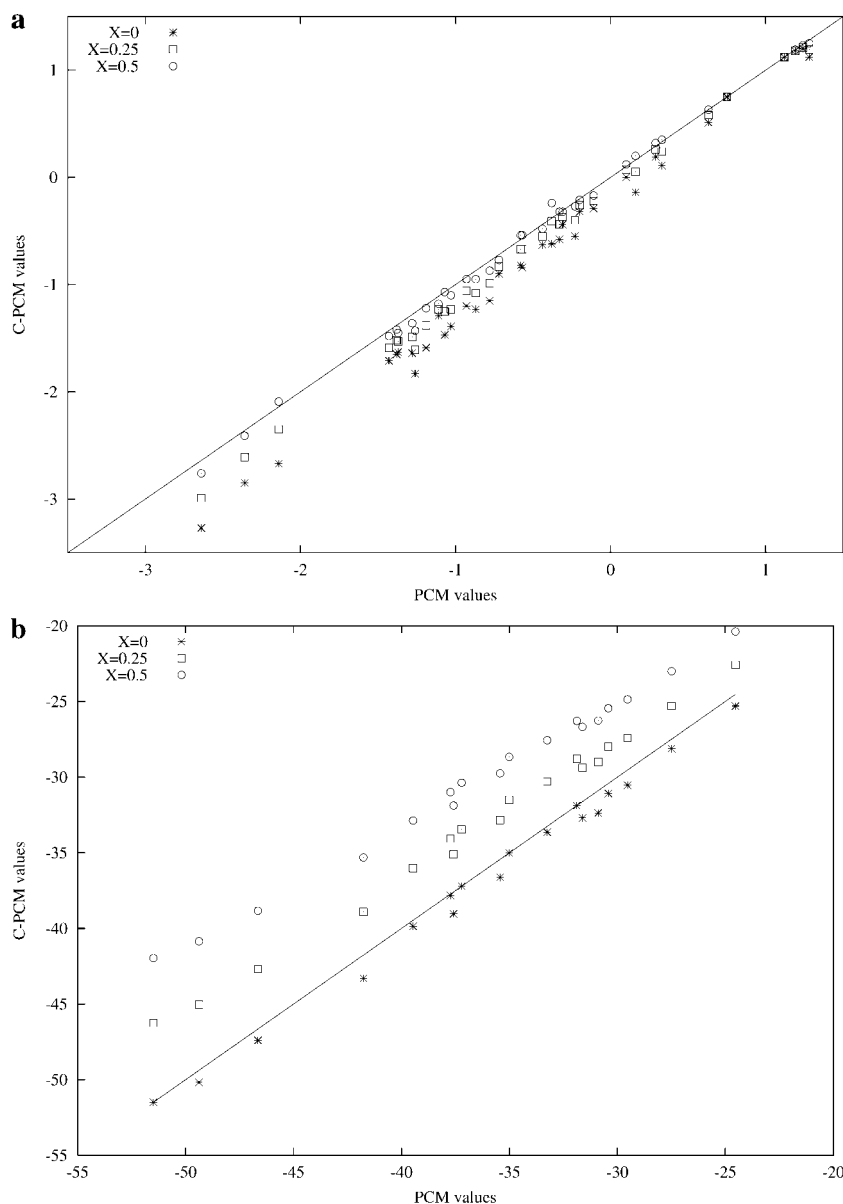


**Figure 3.** Solvation free energy in  $\text{CCl}_4$  for neutral (a) and ionic (b) organic and inorganic solutes, computed at the HF/6-31+G(d) level with C-PCM and different  $X$  values, compared to PCM results.

affect the reliability of the conductor-like model with respect to PCM.

One can see that PCM and C-PCM solvation free energies are practically identical in water, while the agreement is poorer in  $\text{CCl}_4$ , as expected because the conductor picture is weaker for less polar solvents. Moreover, the choice of  $X$  in  $f(\epsilon)$  is irrelevant in polar solvents, but it is important in  $\text{CCl}_4$ . For neutral solutes the best agreement is obtained for  $X = 0.5$ , while for charged molecules it is preferable to use  $X = 0$ . This behavior is consistent with the derivation presented in ref. 9a, where the  $X$  values of 0 and 1 were attributed, respectively, to a dipole and to a point

charge in a single sphere, though in our case the cavities are not simply spherical, and the solvation charges are obtained with a different procedure. Then, to perform C-PCM calculations in non-polar solvents, we suggest selection of the form of  $f(\epsilon)$  according to the solute charge; of course this can be troublesome for solutes that don't have a definite charge, for example a large molecule with one ionic tail. In these cases, one should keep in mind this limitation of the conductor-like model, when nonpolar solvents are involved.

It is also interesting to investigate how the “discretization” process (i.e., representing the solvation charge density as a set of



**Table 1.** Difference between the Total C-PCM Solvation Charge and Gauss' Law Prescription (a.u.) for Extended Polyglycine Chains and Crambin, with Different Tesserae Size.

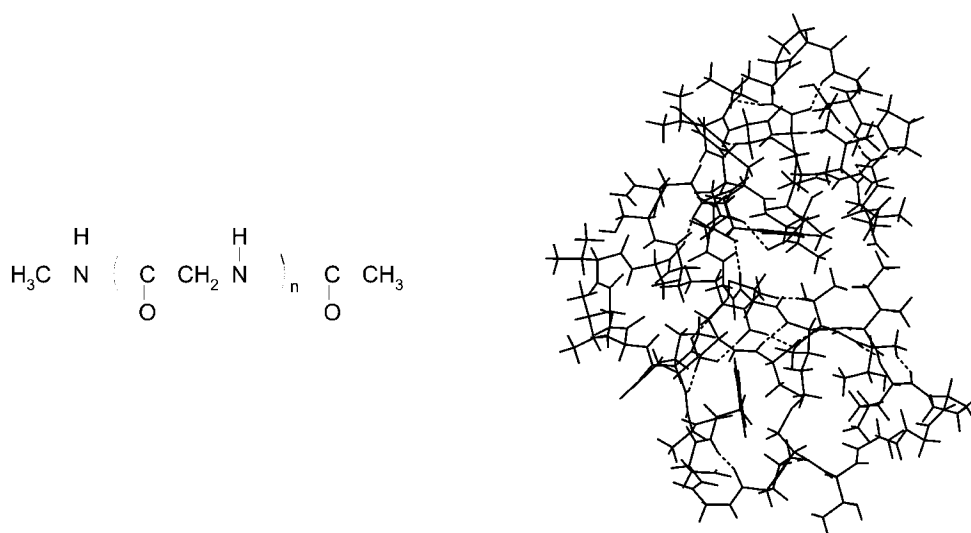
System	Tesserae with average area 0.4 Å <sup>2</sup>		Tesserae with average area 0.2 Å <sup>2</sup>		Tesserae with average area 0.1 Å <sup>2</sup>	
	Number of tesserae	Error	Number of tesserae	Error	Number of tesserae	Error
PG, $n = 3$	1124	-0.00006	2142	-0.00002		
PG, $n = 6$	1838	0.00006	3498	0.00001		
PG, $n = 12$	3268	0.00023	6210	-0.00001		
PG, $n = 24$	6120	0.00052	11634	-0.00004		
PG, $n = 48$	11836	0.00103	22482	0.00004		
PG, $n = 82$	19926	0.00165	37850	-0.00010		
Crambin	13339	-0.00041	22484	-0.00041	39437	0.00000

point charges) affects C-PCM results. Using point charges is an approximation (unavoidable for cavities of general shape), which is expected to become more and more accurate, reducing the size of surface tesserae. This is particularly important in MM calculations, which usually involve very large solutes, so that it is convenient to use not too small tesserae, in order to limit their total number. On the other hand, in MM calculations we know that there is no outlying charge, so that we can use Gauss' law [eq. (4)] as a test for the total computed solvation charge. In Table 1 we list the errors of total solvation charge with respect to Gauss' law for a number of model systems described with AMBER force field.<sup>39</sup> We used a series of rodlike polyglycine (PG) chains in fully extended conformation, and a more globular system, namely crambin (see Fig. 4).

One can see that C-PCM errors are extremely small, even for very large solutes. Such errors reduce further by halving the average size of tesserae, but the default value of 0.4 Å<sup>2</sup> provides

completely satisfactory results. Incidentally, we note that the dielectric version of PCM provides larger errors on these systems (up to two orders of magnitude). Anyway, the discrepancies with respect to Gauss' law are small enough to ensure that the discretization procedure is fully reliable both for C-PCM and for PCM.

In all these MM calculations, the solvation charges were obtained with the iterative scheme described above. The convergence behavior was quite different. In fact, the DIIS procedure converged for the rodlike PG chains, while for crambin it was not able to converge. In this case, it was necessary to use the conjugate gradient procedure, adding a proper preconditioning step to each iteration. We tested different forms for the preconditioning matrix  $\mathbf{M}$  [eq. (24)], namely: (a) the unit matrix (i.e., without preconditioning), (b) the diagonal part of  $\mathbf{S}$ , or (c) a block-factorized  $\mathbf{S}$  matrix, in which only the interactions between tesserae belonging to the same sphere were considered. Procedure (a) did not converge, while (b) and (c) succeeded, the latter being markedly faster

**Figure 4.** Structure of the polyglycine chain (used in fully extended conformation, i.e., with all the peptide angles  $\phi = \psi = 180^\circ$ ), and of crambin protein.

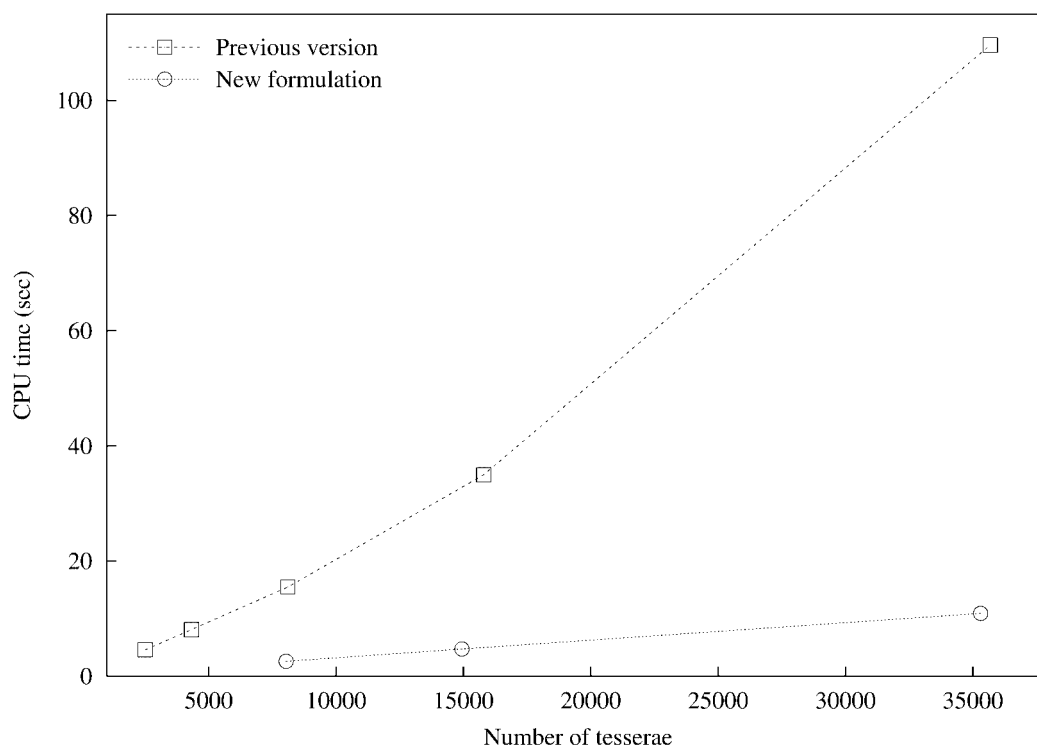


**Figure 5.** CPU times (seconds) for the building of the solute cavity around the polyglycine chains (in fully extended conformation).

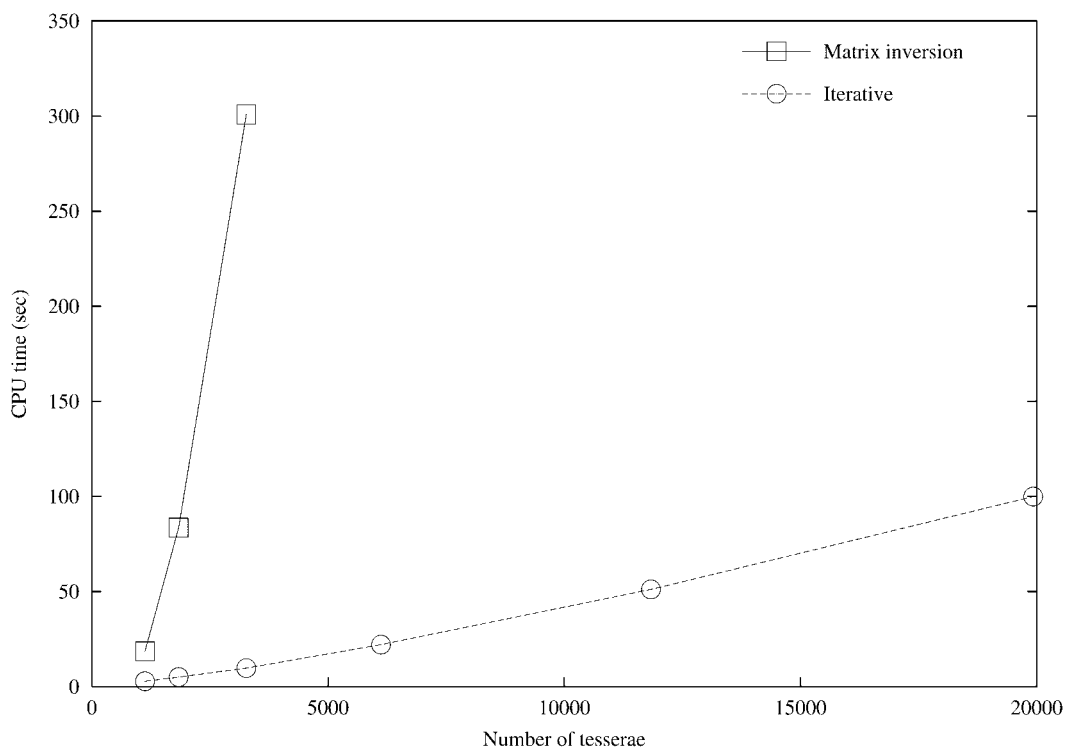


**Figure 6.** CPU times (seconds) for the calculation of C-PCM solvation charges for the polyglycine chains, both with matrix inversion and with iterative approaches.

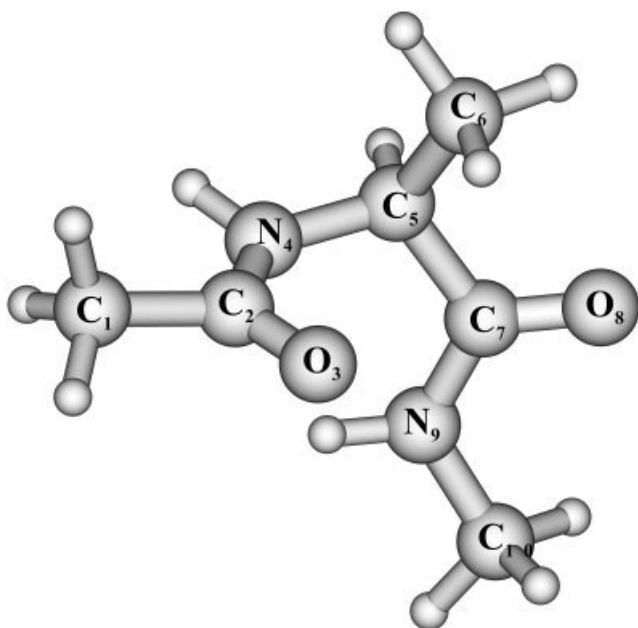


**Figure 7.** Structure and atom numbering of the alanine dipeptide analogue, in the conformation optimized *in vacuo*.

(30% less iterations, and about 20% of time saving). The problem of C-PCM convergence for large iterative calculations will be further analyzed in a forthcoming article. For the moment our recommended approach is the CG procedure with preconditioning (c).

It is also of great interest to look at the computational times needed to build the cavity and to compute the solvation charges for such very large systems. In Figure 5 we compare the time spent for the cavity definition by the previous and the present versions of the code.<sup>24</sup> One can see that the present formulation allows for a dramatic decrease of computational time. Even better results are obtained by the iterative procedure with respect to the matrix inversion approach (see Iterative Solution and Linear Scaling sections). In Figure 6 one can see that the CPU times for matrix inversion become quickly so high that the calculation is practically impossible (in fact, their growth is cubic with the number of tesserae). On the other hand, the iterative approach requires much smaller CPU times, ensuring an almost linear scaling with the number of tesserae. Realistic biochemical systems can be studied only with this approach.

We have described above the analytical algorithms for the calculation of gradients and second derivatives. The best internal test for such procedures is the comparison with the corresponding numerical results. To do that, the C-PCM free energy in solution is computed at a given geometry and then recomputed after very small displacements (of the order of  $10^{-4}$  Å, positive and negative) of all the nuclear coordinates. The energy first and second derivatives are then computed as finite differences. This comparison has been carried out on the alanine dipeptide analogue shown in Figure 7. First, its geometry has been optimized *in vacuo* at the DFT level, with the PBE0 functional and the 6-31+G(d) basis set, reaching one of the stable conformations for this molecule, usually called  $\alpha_D$  and characterized by the peptide angles  $\phi = 71.05^\circ$ ,  $\psi = 19.86^\circ$ . At this geometry, we have computed the free energy gradients in water, both analytically and numerically. The results are compared in Figure 8. One can see that there is a perfect

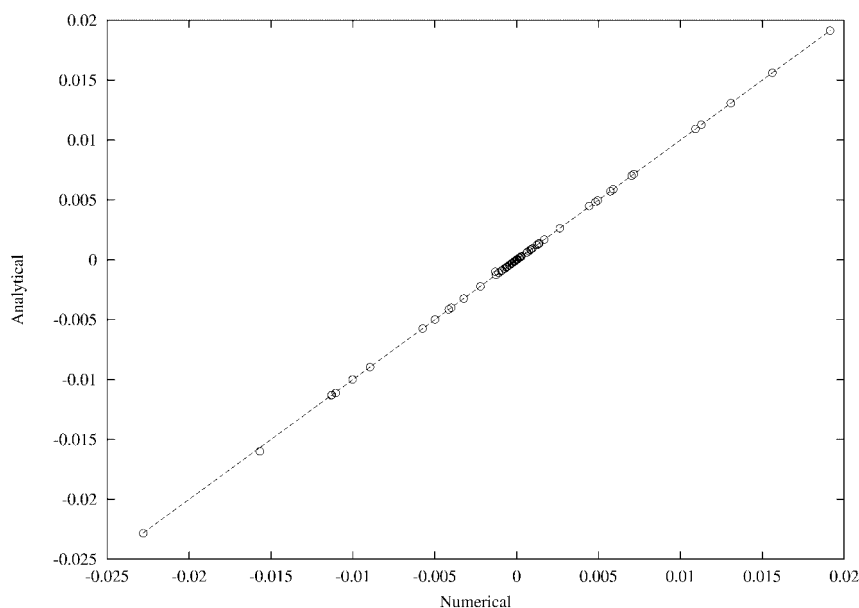


**Figure 8.** Comparison between analytical and numerical energy gradients for the alanine dipeptide analogue at the geometry optimized *in vacuo*, computed in water with C-PCM at the PBE0/6-31+G(d) level.

**Table 2.** Acetone Isotropic Nuclear Shielding Constants (p.p.m.) Computed with GIAO Procedure *In Vacuo* and in Water, Including Zero Order Polarization Only, and with All the C-PCM Contributions.

	Solvent		
	Vacuum	Polarization only	Complete C-PCM contribution
C (Carbonyl)	-2.13	-15.63	-10.55
O	-292.81	-162.10	-235.06
C <sup>α</sup> (Average)	167.06	164.87	166.36
H (Average)	29.51	29.44	29.29

agreement between analytical and numerical gradients, and the same agreement is found in all the tests we have performed. These gradients can be used to reoptimize the alanine dipeptide geometry in water. We found another minimum, with  $\phi = 61.77^\circ$ ,  $\psi = 39.67^\circ$ . The harmonic frequencies in the presence of the solvent were computed at this geometry, and they resulted all positive, confirming that it is a true minimum.

Finally, we performed some test calculations in order to estimate the relative importance of the different C-PCM contributions to electronic properties, that is, the “zero order” solute polarization and the solvent term in density differentiation procedures (see the Electronic Properties section). The system was acetone in water, studied at the PBE0/6-31+G(d,p) level. We computed the solvent effect on the  $n \rightarrow \pi^*$  electronic vertical transition (with TD-DFT approach) and on the isotropic nuclear shielding constants (with GIAO procedure). We stress that this is only a test of the C-PCM procedure. To obtain a quantitative estimate of solvent effects on these properties a more accurate analysis would be necessary, for instance including specific interactions due to the first solvation shell. As for the  $n \rightarrow \pi^*$  transition, we found a value of 4.4549 eV *in vacuo*, with a blue shift in water. The solvent effect was 0.1604 eV (1294  $\text{cm}^{-1}$ ) including the polarization only, 0.1477 eV (1191  $\text{cm}^{-1}$ ) considering also the C-PCM term in the TD-DFT equations, and 0.1550 eV (1250  $\text{cm}^{-1}$ ) including nonequilibrium effects. The solvent effects on NMR constants are collected in Table 2. These results show that both C-PCM contributions are important in the calculation, and neither can be neglected, at least for such applications. Note that also nonequilibrium effects in TD-DFT calculations have similar effects, so that they must be included to obtain accurate results.

## Conclusions

The conductor-like continuum model of solvation, introduced some years ago, has spread in the scientific community due to its accuracy and the relative simplicity of the expressions involved in the definition of the solvent reaction field. The most complete implementation has been realized following the same scheme used for the dielectric model, namely PCM. In this work we have reported on very recent extensions and improvements of the C-

PCM procedure, both from the point of view of the algorithms and of the implementation. The main developments are:

- A new expression for first and second derivatives of the free energy in solution, avoiding the approximations included in the previous formulations.
- The indication that the C-PCM solvation charges should not be corrected according to Gauss' law, because the method can be written as a limit case of the dielectric approach with implicit inclusion of outlying charge effects.
- An effective procedure for the iterative solution of the electrostatic problem in very large systems.
- The reformulation of all the equations in order to use the FMM procedure and to ensure linear scaling of the CPU time with the size of the solute.
- The possibility of performing calculations of electronic properties that involve coupled-perturbed procedure, including all the solvent contributions.

## References

1. Reichardt, C. *Solvents and Solvent Effects in Organic Chemistry* 2nd ed.; VCH: Weinheim, 1990.
2. Rivail, J. L.; Rinaldi, D.; Ruiz-Lopez, M. F. In *Liquid State Quantum Chemistry in Computational Chemistry: Review of Current Trends*; Leszczynski, J., Ed.; World Scientific: Singapore, 1995; p 65.
3. Cramer, C. J.; Truhlar, D. G., In *Solvent Effects and Chemical Reactivity*; Tapia, O.; Bertrán, J., Ed.; Kluwer: Dordrecht, 1996; p 1.
4. Adamo, C.; Cossi, M.; Rega, N.; Barone, V., In *Theoretical Biochemistry: Processes and Properties of Biological Systems*; Erikson, L. A., Ed.; Elsevier Science: Amsterdam, 2001; p 467.
5. Tomasi, J.; Persico, M. *Chem Rev* 1994, 94, 2027.
6. Cramer, C. J.; Truhlar, D. G. *Chem Rev* 1999, 99, 2161.
7. (a) Li, J.; Zhu, T.; Cramer, C. J.; Truhlar, D. G. *J Phys Chem A* 2000, 104, 2178; (b) Dolney, D. M.; Hawkins, G. D.; Winget, P.; Liotard, D. A.; Cramer, C. J.; Truhlar, D. G. *J Comp Chem* 2000, 21, 340.
8. (a) Miertuš, S.; Scrocco, E.; Tomasi, J. *Chem Phys* 1981, 55, 117; (b) Cammi, R.; Tomasi, J. *J Comp Chem* 1995, 16, 1449; (c) Cossi, M.; Barone, V.; Cammi, R.; Tomasi, J. *Chem Phys Lett* 1996, 255, 327; (d) Amovilli, C.; Barone, V.; Cammi, R.; Cancès, E.; Cossi, M.; Mennucci, B.; Pomelli, C. S.; Tomasi, J. *Adv Quantum Chem* 1998, 32, 227.
9. (a) Klamt, A.; Schüürmann, G. *J Chem Soc Perkin 2 Trans* 1993, 799; (b) Klamt, A.; Jonas, V. *J Chem Phys* 1996, 105, 9972; (c) Baldrige, K.; Klamt, A. *J Chem Phys* 1997, 106, 66622; (d) Schüürmann, G. *J Chem Phys* 1998, 109, 9523; (e) Schäfer, A.; Klamt, A.; Sattel, D.; Lohrenz, J. C. W.; Eckert, F. *Phys Chem Chem Phys* 2000, 2, 2187.
10. (a) Truong, T. N.; Stefanovich, E. V. *Chem Phys Lett* 1995, 240, 253; (b) Truong, T. N.; Nguyen, U. N.; Stefanovich, E. V. *Int J Quantum Chem* 1996, 30, 403.
11. Barone, V.; Cossi, M. *J Phys Chem A* 1998, 102, 1995.
12. (a) Klamt, A. *J Phys Chem A* 1998, 102, 5057; (b) Klamt, A.; Eckert, F. *Fluid Phase Equil* 2000, 172, 43; (c) Klamt, A., In *Encyclopedia of Computational Chemistry*; Schleyer, P. v. R.; Allinger, L., Eds.; Wiley: New York, 1998; p 604.
13. Pye, C. C.; Ziegler, T. *Theor Chem Acc* 1999, 101, 396.
14. (a) Cancès, E.; Mennucci, B.; Tomasi, J. *J Chem Phys* 1997, 107, 3032; (b) Mennucci, B.; Cancès, E.; Tomasi, J. *J Phys Chem B* 1997, 101, 10506; (c) Cossi, M.; Barone, V. *J Chem Phys* 1998, 109, 6246; (d) Mennucci, B.; Cammi, R.; Tomasi, J. *J Chem Phys* 1999, 110,

- 6858; (e) Cammi, R.; Mennucci, B. *J Chem Phys* 1999, 110, 9877; (f) Cossi, M.; Barone, V. *J Chem Phys* 2001, 115, 4708; (g) Cossi, M.; Rega, N.; Scalmani, G.; Barone, V. *J Chem Phys* 2001, 114, 5691.
15. Cossi, M.; Scalmani, G.; Rega, N.; Barone, V. *J Chem Phys*. In press.
16. Cossi, M.; Mennucci, B.; Pitarch, J.; Tomasi, J. *J Comput Chem* 1998, 19, 833.
17. Chipman, D. M. *J Chem Phys* 2000, 112, 5558.
18. (a) Strain, M. C.; Scuseria, G. E.; Frisch, M. J. *Science* 1996, 271, 51; (b) White, C. A.; Johnson, B. G.; Gill, P. M. W.; Head-Gordon, M. *Chem Phys Lett* 1996, 253, 268; (c) Svensson, M.; Humbel, S.; Froese, R. D. J.; Matsubara, T.; Sieber, S.; Morokuma, K. *J Phys Chem* 1996, 100, 19375.
19. (a) Reiss, H.; Frisch, H. L.; Lebowitz, J. L. *J Chem Phys* 1959, 31, 369; (b) Pierotti, R. A. *Chem Rev* 1976, 76, 717.
20. (a) Caillet, J.; Claverie, P.; Pullman, B. *Acta Cryst* 1978, B34, 3266; (b) Floris, F. M.; Tomasi, J. *J Comp Chem* 1989, 10, 616; (c) Floris, F. M.; Tomasi, J.; Pascual-Ahuir, J.-L. *J Comp Chem* 1991, 12, 784.
21. Frisch, M. J.; Trucks, G. W.; Schlegel, H. B.; Scuseria, G. E.; Robb, M. A.; Cheeseman, J. R.; Zakrzewski, V. G.; Montgomery, J. A. Jr; Kudin, K. N.; Burant, J. C.; Millam, J. M.; Stratmann, R. E.; Tomasi, J.; Barone, V.; Mennucci, B.; Cossi, M.; Scalmani, G.; Rega, N.; Iyengar, S.; Petersson, G. A.; Ehara, M.; Toyota, K.; Nakatsuji, H.; Adamo, C.; Jaramillo, J.; Cammi, R.; Pomelli, C.; Ochterski, J.; Ayala, P. Y.; Morokuma, K.; Salvador, P.; Dannenberg, J. J.; Dapprich, S.; Daniels, A. D.; Strain, M. C.; Farkas, O.; Malick, D. K.; Rabuck, A. D.; Raghavachari, K.; Foresman, J. B.; Ortiz, J. V.; Cui, Q.; Baboul, A. G.; Clifford, S.; Cioslowski, J.; Stefanov, B. B.; Liu, G.; Liashenko, A.; Piskorz, P.; Komaromi, I.; Gomperts, R.; Martin, R. L.; Fox, D. J.; Keith, T.; Al-Laham, M. A.; Peng, C. Y.; Nanayakkara, A.; Challacombe, M.; Gill, P. M. W.; Johnson, B.; Chen, W.; Wong, M. W.; Andres, J. L.; Gonzalez, C.; Head-Gordon, M.; Replogle, E. S.; Pople, J. A. *Gaussian 01, Development Version (Revision B.01)*; Gaussian, Inc.: Pittsburgh, PA, 2001.
22. Pascual-Ahuir, J.-L.; Silla, E.; Tuñon, I. *J Comput Chem* 1994, 15, 1127.
23. Cossi, M.; Mennucci, B.; Cammi, R. *J Comput Chem* 1996, 17, 57.
24. Scalmani, G.; Barone, V. In preparation.
25. McWeeny, R. *Methods of Molecular Quantum Mechanics*, 2nd ed.; Academic Press: London, 1992.
26. Runge, E.; Gross, E. K. U. *Phys Rev Lett* 1984, 52, 997.
27. Casida, M. K., In *Recent Advances in Density Functional Methods, Part I*; Chong, D. P., Ed.; World Scientific: Singapore, 1995; p 155.
28. Petersilka, M.; Gossmann, U. J.; Gross, E. K. U. *Phys Rev Lett* 1996, 76, 1212.
29. (a) Bonaccorsi, R.; Cimiraglia, R.; Tomasi, J. *J Comp Chem* 1983, 4, 567; (b) Aguilar, M. A.; Olivares del Valle, F. J.; Tomasi, J. *J Chem Phys* 1993, 98, 7375; (c) Cammi, R.; Tomasi, J. *Int J Quantum Chem: Quantum Chem Symp* 1995, 29, 465; (d) Mennucci, B.; Cammi, R.; Tomasi, J. *J Chem Phys* 1998, 109, 2798.
30. Klamt, A. *J Phys Chem* 1996, 100, 3349.
31. Cossi, M.; Barone, V. *J Chem Phys* 2000, 112, 2427.
32. Wolinski, K.; Hilton, J. F.; Pulay, P. *J Am Chem Soc* 1990, 112, 8251.
33. Pomelli, C. S.; Tomasi, J.; Barone, V. *Theor Chem Acc* 2001, 105, 446.
34. Barrett, R.; Berry, M.; Chan, T. F.; Demmel, J.; Donato, J.; Dongarra, J.; Eijkhout, V.; Pozo, R.; Romine, C.; Van der Vorst, H. *Templates for the Solution of Linear Systems: Building Blocks for Iterative Methods*, 2nd ed.; SIAM: Philadelphia, 1994. (Also available online at [www.netlib.org](http://www.netlib.org))
35. (a) York, D. M.; Lee, T.-S.; Yang, W. *J Chem Phys* 1996, 105, 2744; (b) York, D. M.; Lee, T.-S.; Yang, W. *Chem Phys Lett* 1996, 263, 297; (c) York, D. M.; Lee, T.-S.; Yang, W. *J Am Chem Soc* 1996, 118, 10940.
36. (a) Petersson, G. A.; Al-Laham, M. A. *J Chem Phys* 1991, 94, 6081; (b) Petersson, G. A.; Bennett, A.; Tensfeldt, T. G.; Al-Laham, M. A.; Shirley, W. A.; Mantzaris, J. *J Chem Phys* 1988, 89, 2193.
37. Adamo, C.; Barone, V. *J Chem Phys* 1999, 110, 6158.
38. Barone, V.; Cossi, M.; Tomasi, J. *J Chem Phys* 1997, 107, 3210.
39. Cornell, W. D.; Cieplak, P.; Bayly, C. I.; Gould, I. R.; Merz, K. M. Jr; Ferguson, D. M.; Spellmeyer, D. C.; Fox, T.; Caldwell, J. W.; Kollman, P. A. *J Am Chem Soc* 1995, 117, 5179.